Scaling Relation between Electrical Conductivity Percolation and Water Diffusion Coefficient in Sodium Bis(2-ethylhexyl) Sulfosuccinate-Based Microemulsion

Hiroshi Kataoka,*,† Taro Eguchi,‡ Hirotsugu Masui,§ Keisuke Miyakubo, Hirokazu Nakayama,|| and Nobuo Nakamura⊥

Department of Chemistry, Graduate School of Science, Osaka University, Toyonaka, Osaka 560-0043, Japan

Received: February 25, 2002; In Final Form: September 2, 2003

We investigated the conductivity percolation mechanism of a water-in-oil (W/O) microemulsion composed of sodium bis(2-ethylhexyl) sulfosuccinate (AOT), D_2O, and decane using impedance spectroscopy and the pulsed-gradient spin-echo (PGSE) NMR technique. The electrical conductivity (σ) measured as a function of temperature (T) and the volume fraction (Φ) of water droplets show a marked increase near room temperature. The PGSE NMR measurements show that the water diffusion coefficient (D_{water}) is responsible for σ, implying that the main charge carrier is the cation species (Na^+) dissolved in and transported with water. Given the relation $D_{exchange} \equiv D_{water} - D_{droplet}$, where $D_{exchange}$ and $D_{droplet}$ are diffusion coefficients for the exchange of water between water droplets and for the whole host droplet, respectively, a quantitative scaling relation between reduced conductivity $\sigma T\Phi^{-1}$ and $D_{exchange}$ was first confirmed to show asymptotic behavior in which $\sigma T\Phi^{-1} \sim (D_{exchange})^{\beta}$ [$\beta = 3.2$ for $-10.7 \leq \log (D_{exchange}) \leq -10.0$ and $\beta = 1.3$ for $-10.0 \leq \log (D_{exchange}) \leq -9.3$]. This reveals that a common mechanism governs both conductivity percolation and the water exchange between droplets in AOT-based W/O microemulsion. The discontinuity of the exponent β at $\log (D_{exchange})$ ca. 10.0 indicates a change in the mechanism of water exchange between the droplets, resulting mainly from Na cation distribution in a droplet.

Introduction

Three-component water-in-oil (W/O) microemulsions comprising water, oil, and an ionic surfactant have been target materials for experimental and theoretical studies of the percolation phenomenon observed in measurements of electrical conductivity (σ) of these systems.[1] Among the various systems, a sodium bis(2-ethylhexyl) sulfosuccinate (AOT)-based W/O microemulsion has been studied extensively[2−14] because of its novel phase diagram.[5,12] At or near room temperature, it forms a transparent one-phase microemulsion (L_2 phase) in which water cores coated by a single layer of AOT molecules are dispersed in a continuous decane phase over wide ranges of both temperature (T) and the volume fraction of the water droplets (Φ).[5,12] A sharp increase in specific electrical conductivity (σ/Φ) from 10^{-7} to 10^{-2} S cm^{-1} occurs in a narrow temperature range with no change in droplet structure.[15−19]

This critical behavior has been understood to be a percolation phenomenon associated with the formation of conducting paths for charge carriers.[20] From analysis of the critical exponents below and above the percolation point, i.e., the inflection point of conductivity in this case, the conduction property of the microemulsion is classified as a dynamic percolation scheme[21] below the percolation point (T_p) and a static[20] percolation scheme above T_p. Migration of the charged species is inferred to occur through formation of certain static paths in the static case.[20] In the dynamic model, the paths of the charge carriers must vary with time[21] associated with the droplet motion. These models have revealed basic aspects of the conductivity percolation.

In the AOT-based W/O microemulsion, conductivity is attributed to the motion of Na cation dissociated in the water core and the AOT anion having an anionic headgroup SO_3^-.[7] Two models for dominant charge carriers have been proposed. One is that electricity is carried by hopping of the AOT anion from one droplet to another.[17,21−25] Another model addresses the transient fusion of droplets and the associated mass exchange between droplets.[26−29] In that model, electricity is transported by the Na cation through water paths formed temporarily upon collision of the droplets.

Feldman et al.[30] used the pulsed-gradient spin-echo (PGSE) NMR technique to measure self-diffusion coefficients of water, AOT, and decane individually in an H_2O/AOT/decane microemulsion system. They found that water diffusion is responsible for electrical conductivity above and below the percolation threshold, whereas AOT diffusion is related only to percolation of conductance above the percolation threshold.[30] Moreover, the absolute value of the diffusion coefficient of AOT was smaller than that of water above the percolation threshold by a factor of 10.[30] These results indicate that conductivity percolation of the AOT-based W/O microemulsion is related to the Na cation dissolved in the droplet's water core. The main mechanism of electrical conductivity is inferred to be the exchange of the solute between droplets through water channels that emerge spontaneously from droplet collision.

However, Feldman et al. examined an AOT-based W/O microemulsion system with only one composition;[30] therefore it remains questionable whether Na cation acts as the dominant

* To whom correspondence should be addressed at the Faculty of Education, Toyama University, 3190 Gofuku, Toyama 930-8555, Japan. Fax +81-76-445-6264; e-mail kataokah@edu.toyama-u.ac.jp.

† Present address: Toyama University, Toyama 930-8555, Japan.

‡ Present address: The Museum of Osaka University, Toyonaka 560-0043, Japan.

§ Present address: HITEC Co., Ltd., Osaka 530-6025, Japan.

|| Present address: Kobe Pharmaceutical University, Kobe 658-8588, Japan.

⊥ Present address: Shinshu University, Matsumoto 390-8621, Japan.

10.1021/jp020510a CCC: $25.00
Published on Web 10/18/2003

charge carrier over the entire region of the compositions. The present study is intended to show the relation between water dynamics and electrical conductivity over the wide region of the AOT-based W/O microemulsion and to clarify the mechanism of conductivity percolation. We studied the L_2 phase of a D_2O/AOT/decane ($[D_2O]/[AOT] = 40.8$) system in which the structure model and phase diagram have been established, thereby avoiding ambiguity that might originate from a wide variety of microemulsions.[9−12] We conducted experiments for electrical conductivity and diffusion coefficients of water, AOT, and decane using impedance measurements and the PGSE-NMR technique, respectively.

Experimental Section

All materials were from commercial sources: AOT [sodium bis(2-ethylhexyl) sulfosuccinate; Tokyo Kasei Kogyo Co., Ltd.] was purified according to the literature.[31] Decane (Wako Pure Chemical Industries, Ltd.) was dried with molecular sieves and distilled before use; D_2O (99.9 at. % D; Aldrich Chemical Co., Inc.) was used without further purification. The D_2O/AOT/decane microemulsion was prepared by mixing appropriate amounts of D_2O, AOT, and decane in a glass flask. The volume fraction of water droplets Φ in the system was defined as $\Phi = \Phi_{D_2O} + \Phi_{AOT}$, where Φ_{D_2O} and Φ_{AOT} denote volume fractions of D_2O and AOT, respectively, assuming that the density of AOT in the microemulsion was equal to that in the bulk solid.[10] The molar ratio of water to surfactant, $[D_2O]/[AOT]$, was fixed at 40.8 in all samples. Hydrolysis of the AOT molecule to 2-ethylhexanol[10] was checked with the ^{1}H NMR spectrum. No signal resulting from hydrolysis was detected in the fresh sample used in this work.

Electrical conductivity was measured with a Hewlett-Packard 4276A LCZ meter in the range between 100 Hz and 20 kHz. Temperatures were measured to 288−323 K and controlled to within ±0.1 K by Chromel-P−Constantan thermocouples.

A Varian Unity 600 spectrometer operating at the ^{1}H Larmor frequency of 599.9 MHz was used for PGSE-NMR experiments. Proton concentration in D_2O, about 0.1%, was sufficient to detect the NMR signal with a high signal-to-noise ratio. The water proton signal was observed at 4.5 ppm. The signals of $-CH_2$ at 1.5 ppm and $-CH_3$ groups at 1.0 ppm of AOT and decane were overlapped as indicated in some references.[32,33] The self-diffusion coefficient of water was determined by use of the Stejskal−Tanner sequence[34] in which the echo amplitude $M(2\tau)$ is given as $M(2\tau) \propto \exp[-\gamma^2\delta^2g^2D(\Delta - \delta/3)]$, where γ is the gyromagnetic ratio, δ is the width of the field gradient pulse, g is the magnitude of the field gradient, and Δ is the time separation between the two gradient pulses. Measurements were done by varying δ between 0.316 and 14.0 ms under conditions in which $\Delta = 0.600$ s and $g = 0.195$ T m^{-1}. A typical $\pi/2$ pulse width was 10 μs at room temperature. The sample temperature was controlled to within ±0.1 K during measurements. The semilog plot of the echo amplitude of the water proton at 4.5 ppm against $\gamma^2\delta^2g^2(\Delta - \delta/3)$ shows a linear relation within experimental error, so that a single diffusion coefficient (D_{water}) was obtained for each composition throughout the temperature range of measurements. Diffusion coefficients of AOT and decane were obtained from semilog plots of the echo amplitudes of the $-CH_2$ and $-CH_3$ groups, which showed a superposition of two exponential decays as $M(2\tau) \propto a \exp[-\gamma^2\delta^2g^2D_{decane}(\Delta - \delta/3)] + b \exp[-\gamma^2\delta^2g^2D_{AOT}(\Delta - \delta/3)]$, where a and b are experimental parameters. The faster diffusion coefficient was assigned to that of decane and the slower one to that of AOT, as in ref 30.

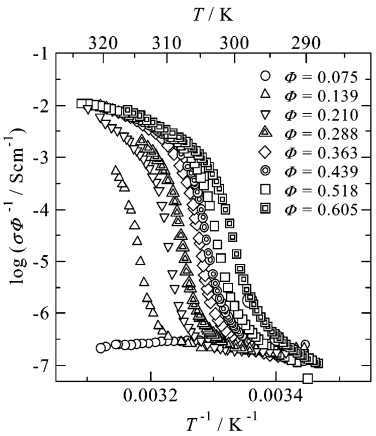

Figure 1. Temperature dependence of specific conductivity σ/Φ in the D_2O/AOT/decane system ($[D_2O]/[AOT] = 40.8$) at an applied frequency of 100 Hz.

Results and Discussion

Electrical Conductivity Measurements. Figure 1 shows the specific conductivity (σ/Φ) of the D_2O/AOT/decane microemulsion at an applied frequency of 100 Hz in the temperature range between 288 and 323 K. A sharp increase in σ/Φ by a factor of 10^5 from 10^{-7} to 10^{-2} S cm^{-1} was observed at every volume fraction except at $\Phi = 0.075$, as in the case of the H_2O/AOT/decane system.[18] The increase in σ was characterized by the power law:

$$\sigma \propto (T_p - T)^{-s} \quad \text{for } T < T_p \tag{1a}$$

and

$$\sigma \propto (T - T_p)^{\mu} \quad \text{for } T > T_p \tag{1b}$$

where T is the absolute temperature, T_p is the percolation temperature, which is defined as the inflection point of the sigmoid curve,[15,17,18,35] and s and μ are critical exponents. The critical point at which an infinite cluster percolates for the first time through an infinite lattice with a finite probability is theoretically defined as T_p.[36] Physically, it is assigned to the temperature or the volume fraction of the water droplets at which a conductive path spreads over the whole system for the first time. Figure 2 represents power-law behavior observed in the close vicinity of T_p. Table 1 lists critical exponents s and μ and T_p. Values of μ at all Φ values are consistent with the static percolation model,[20] which postulates that $\mu = 2.0$. As for exponent s, the values 1.1 to 1.6 agree with 1.35, which is predicted by the dynamic model.[21]

Figure 3 shows the phase diagram obtained in the present work. The upper limit of the L_2 phase agrees well with a previous report for the D_2O/AOT/decane system.[37] Isotope effects between the D_2O and H_2O systems were detected at the phase boundaries. On the percolation curve, the D_2O system shows a decrease of 3 K compared to the H_2O system.[19] The D_2O system shows an increase of 5−10 K for the clearing point curve between the one-phase and two-phase regions compared to those in the H_2O system.[37] This also concurs with the literature.[38]

Dynamic Behavior of Water, AOT, and Decane in the Microemulsion. Diffusion coefficients of water, AOT, and decane in the L_2 phase were measured by the PGSE-NMR technique to examine conductivity percolation in relation to dynamics and structure of water droplets. Short spin−spin relaxation time of ^{23}Na−NMR signals prevents measurement

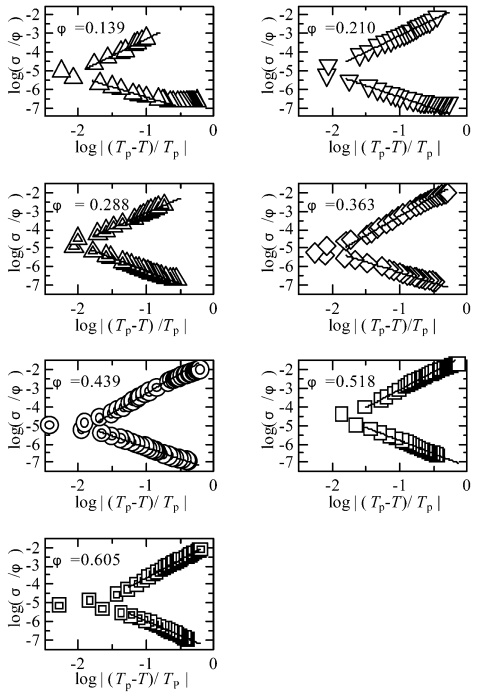

Figure 2. Critical behavior of electrical conductivity below and above percolation threshold T_p.

TABLE 1: Percolation Threshold T_p and Critical Exponents of σ below T_p (s) and above T_p (μ) at Each Φ

Φ	T_p/K	s	μ
0.139	313.9 ± 0.3	1.1 ± 0.1	1.9 ± 0.2
0.210	309.5 ± 0.3	1.2 ± 0.2	1.8 ± 0.2
0.288	307.6 ± 0.3	1.3 ± 0.1	1.8 ± 0.2
0.363	304.5 ± 0.2	1.2 ± 0.1	2.0 ± 0.1
0.439	303.4 ± 0.4	1.3 ± 0.3	1.9 ± 0.1
0.518	302.0 ± 0.4	1.5 ± 0.2	1.9 ± 0.2
0.605	299.3 ± 0.3	1.6 ± 0.2	1.9 ± 0.2

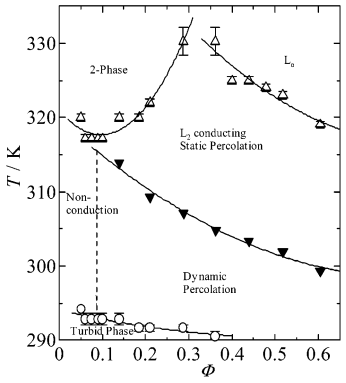

Figure 3. $T-\Phi$ phase diagram of the D_2O/AOT/decane microemulsion. Borderlines are a visual guide.

of diffusion coefficient of the Na cation. Therefore, the diffusion coefficient of the residual water protons in D_2O was used as a reference for mobility of the Na cation dissolved in water and transported with solvated water molecules.

Figure 4 shows temperature dependence of diffusion coefficients of water (D_{water}), AOT (D_{AOT}), and decane (D_{decane}) at water droplet volume fractions of Φ = 0.075, 0.139, 0.287, 0.361, and 0.605. Values for D_{decane} at all Φs show a temperature dependence of an Arrhenius type with activation energy of 12 ± 2 kJ mol^{-1}. On the other hand, D_{water} and D_{AOT} exhibit non-Arrhenius temperature dependencies. Figure 5 shows a typical case (Φ = 0.361) with σ. The onset of D_{water} (292 K)

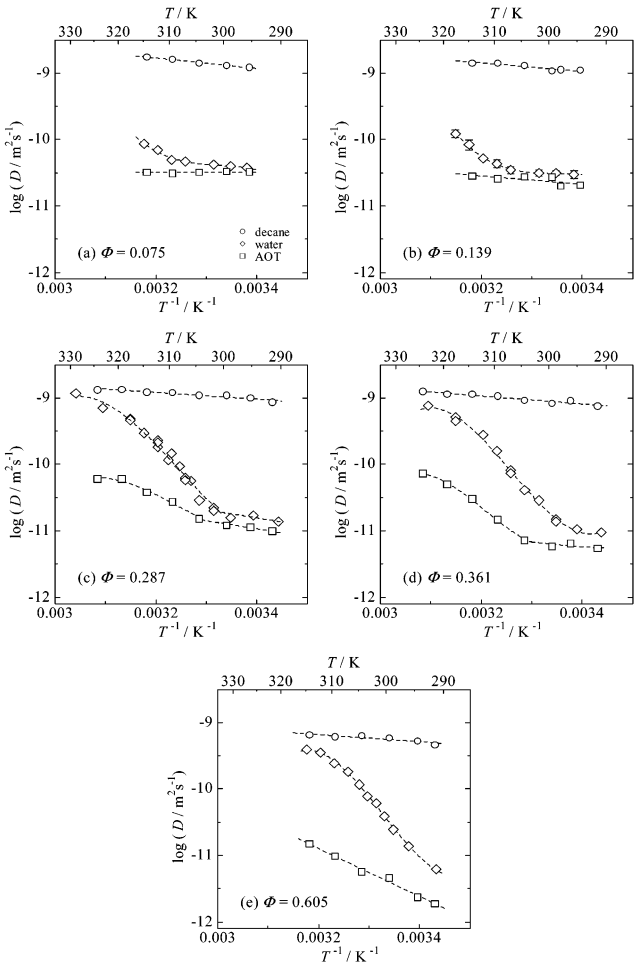

Figure 4. Temperature dependence of self-diffusion coefficients of water (D_{water}, ◇), AOT (D_{AOT}, □), and decane (D_{decane}, ○) in the D_2O/AOT/decane system at [D_2O]/[AOT] = 40.8 with various volume fractions of water droplets Φ. Broken lines are visual guides.

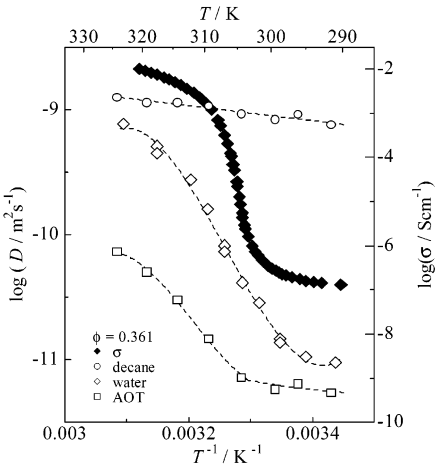

Figure 5. Temperature dependence of the specific conductivity (σ/Φ) and the self-diffusion coefficients of water, AOT, and decane at Φ = 0.361: the broken lines are visual guides.

coincides with that of σ, whereas that of D_{AOT} (302 K) is 10 K higher than those of D_{water} and σ. A similar result has been reported for a H_2O/AOT/decane system of [H_2O]/[AOT] = 26.3.[30] Further, the value of D_{water} is 10 times higher than that of D_{AOT} at 335 K above T_p. These results suggest that diffusion of water is a more important factor in conductivity percolation than the AOT anion, thus suggesting that Na cation dissolved

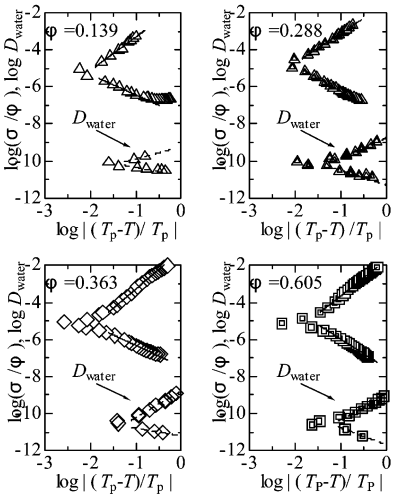

Figure 6. Critical behavior of the self-diffusion coefficient of water (lower) and electrical conductivity σ (upper) in the D_2O/AOT/decane system in the vicinity of the percolation temperature T_p of σ.

in the water plays a dominant role in conductivity percolation as a charge carrier.

The contribution of ions to σ in this system is described as $\sigma = \sigma_{Na} + \sigma_{AOT}$, where σ_{Na} and σ_{AOT} are conductivities resulting from the Na cation and AOT anion, respectively. In general, electrical conductivity (σ) can be associated with the charge carrier mobility (μ) as

$$\sigma = cFz\mu \tag{2}$$

where c is the charge carrier concentration, F is the Faraday constant, and z is the charge number. Mobility (μ) and diffusion coefficient (D) are related by the Einstein relation:

$$D = \mu RT/zF \tag{3}$$

where R is the gas constant. Therefore, the specific conductivity engendered by the AOT anion (σ_{AOT}/Φ) could be written as

$$\sigma_{AOT}/\Phi = (c/\Phi)F^2 z_{AOT}{}^2 D_{AOT}/RT \tag{4}$$

Provided that the degree of dissociation of AOT molecules (x) is 1 ($c/\Phi = 8.84 \times 10^2$ mol m^{-3}) and using the value of $D_{AOT} = 7 \times 10^{-11}$ m^2 s^{-1}, eq 4 yields $\sigma_{AOT}/\Phi = 2.1 \times 10^{-3}$ S cm^{-1} for $\Phi = 0.361$ and $T = 325$ K. This value is 21% of the total specific conductivity ($\sigma/\Phi = 1 \times 10^{-2}$ Scm^{-1}), so that the contribution of the Na cation to σ/Φ is estimated as $\sigma_{Na}/\Phi = 7.9 \times 10^{-3}$ Scm^{-1}, which is 79% of σ/Φ and 3.5 times that of the AOT anion. When $x < 1$, the Na cation contribution to total conductivity will be greater than 79%. By use of the value of $x = 0.3$, which is suggested by ^{23}Na-NMR spectroscopy,[32] the above estimation yields σ_{Na}/Φ to be 15 times σ_{AOT}/Φ. In addition, the molecular weight of an AOT anion (421.47) is 18 times heavier than that of a Na cation (22.99); therefore it is reasonable to infer that Na cation mobility is greater than AOT anion mobility. We conclude that the dominant charge carrier in conductivity percolation is the Na cation. Although we recognize the small contribution AOT anion has to total conductivity, we will focus subsequent study on the relation between electrical conductivity and water diffusion to examine the percolation mechanism in more detail.

Diffusion Behavior of Water Proton. Figure 6 shows critical behavior of D_{water} and σ around T_p of σ. Table 2 summarizes the power-law behavior of D_{water}. Neither exponent for D_{water} coincided with those of σ. This implies that PGSE-NMR observes a different aspect of the conductivity percolation phenomenon from that obtained by conductivity measurements.

TABLE 2: Critical Exponents for D_{water} below T_p (s) and above T_p (μ) at Each Φ Estimated by D_{water} Measurements[a]

Φ	T_p/K	s	μ
0.139	313.9 ± 0.3	0.5	0.6
0.288	307.6 ± 0.3	0.8	1.1
0.363	304.5 ± 0.2	0.4	1.4
0.605	299.3 ± 0.3	0.9	1.2

[a] Values of T_p are determined by electrical conductivity measurements.

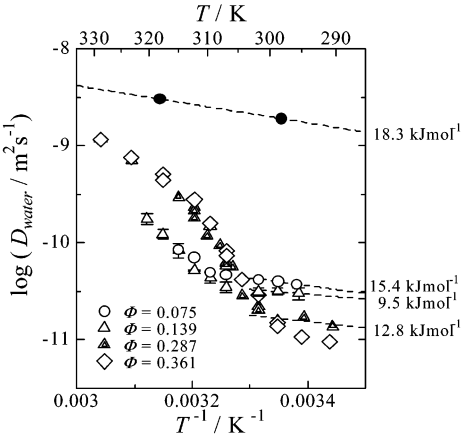

Figure 7. Plot of the self-diffusion coefficient of water protons against temperature in the D_2O/AOT/decane system: from the slopes of the plots, activation energies are estimated at low temperatures. The diffusion coefficient of residual protons near D_2O is also shown (●).[40]

We consider the transport mechanism of water in terms of the droplet structure proposed by scattering experiments; thereby, we elucidate characteristics of D_{water} observed by PGSE-NMR.[10−12,39] The fact that the absolute values of D_{water} in the microemulsion are smaller than that in the bulk water,[40] as plotted in Figure 7, implies that droplet structure slows down the diffusion of water. Hence, D_{water} is represented by three diffusion coefficients: (i) the diffusion coefficient inside a host droplet (D_{inner}), (ii) that for a whole host droplet ($D_{droplet}$), and (iii) that for the contribution of water exchange between droplets ($D_{exchange}$).

(i) Diffusion of Water Molecules inside a Droplet (D_{inner}). Within a droplet, the maximum transport distance of a water molecule is limited to the diameter of the droplet, ca. 12 nm.[7] Provided that the diffusion coefficient of water molecule in a droplet is equal to that in bulk water[40] ($D \sim 2 \times 10^{-9}$ m^2 s^{-1}) it takes only $t \sim (2r)^2/2D = 40$ ns for a water molecule in a droplet to traverse the diameter. In present PGSE experiments with the evolution time for diffusion, $\Delta = 0.600$ s, a water molecule traverses the entire droplet, so the water molecule is regarded as located in the droplet center. Thus we can ignore the effect of D_{inner} on the D_{water}.

(ii) Water Diffusion Associated with the Motion of the Host Droplet ($D_{droplet}$). Far below the inflection point of D_{water}, each D_{water} has weak temperature dependence. However, it decreases almost linearly with an increase in Φ, as shown in Figure 7. This implies that the water molecule motion becomes more restricted as the droplets increase for Φ because Φ is proportional to the number density of the droplets. Figure 7 shows our estimated activation energies with an Arrhenius plot of the D_{water} far below T_p for water motion. Data for $\Phi = 0.361$ were not used because D_{water} began to increase below 296 K for this volume fraction. The estimated activation energies (ca. 12.5 ±

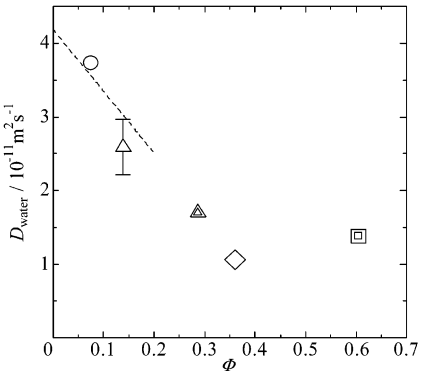

Figure 8. Volume fraction (Φ) dependence of D_{water} in the D_2O/AOT/decane system at 295.2 ± 0.7 K. The broken line shows $D_s = 4.2 \times 10^{-11}(1 - 2\Phi)$.

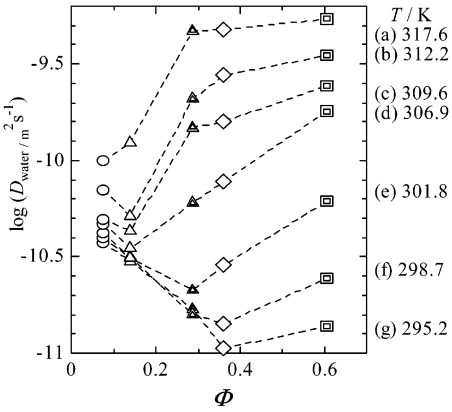

Figure 9. Φ dependence of D_{water} at various temperatures.

3.0 kJ mol^{-1}) are smaller than that for residual protons in bulk D_2O (18.3 kJ mol^{-1}); they almost coincide with that of decane in the present microemulsion (12 ± 2 kJ mol^{-1}) determined by diffusion measurements (Figure 4) and spin−lattice relaxation time measurements.[41] This result concurs with those for other microemulsion systems.[25,30,42,43] Therefore D_{water} far below T_p is identified with $D_{droplet}$ through the medium of decane.

Further evidence for droplet diffusion was given by Φ dependence of D_{water}. For cases where $\Phi \ll 1$, the so-called memory effect[44−46] can be applied to interpret Φ dependence of D_{water}. In the hypothetical case of hard spheres that do not undergo hydrodynamic interaction, the self-diffusion coefficient for mutually interacting Brownian particles is represented as

$$D_{droplet} = D_0(1 - 2\Phi) \tag{5}$$

where D_0 is the diffusion coefficient of a droplet at infinite dilution. Equation 5 predicts a linear decrease in $D_{droplet}$ with an increase in Φ. Figure 8 plots the experimental D_{water} against Φ at 295.2 ± 0.7 K. The least-squares fitting of experimental data for Φ = 0.075 and 0.139 to eq 5, shown by a broken line, yields $D_0 = 4.2 \times 10^{-11}$ m^2 s^{-1}. Applying the Stokes−Einstein equation $D = kT/6\pi\eta r$, where k is the Boltzmann constant, η is the viscosity of decane (9.0×10^{-4} Pa·s),[47] and r is the radius of the droplet, we obtain $r = 6$ nm, which agrees with the small-angle neutron scattering (SANS) experiment results.[7,38] Thus D_{water} at Φ = 0.075 and 0.139 at 295.2 K was identified as $D_{droplet}$.

(iii) Effect of the Exchange of Water Molecules between Droplets ($D_{exchange}$). Figure 9 displays the Φ dependence of

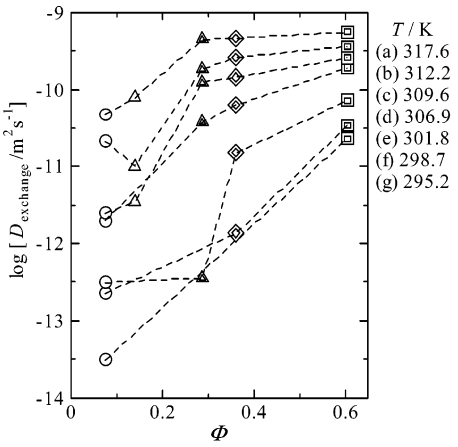

Figure 10. Φ dependence of $D_{exchange}$ at various temperatures.

D_{water}. For $T < 302$ K and $\Phi < 0.4$, D_{water} decreases with an increase in Φ. In this region, Brownian motion of a droplet occurs simply. On the other hand, a further increase in Φ engenders an increase in D_{water}, suggesting the setting up of another motion of water that is associated with the percolation phenomenon. A probable candidate for such a mechanism of water motion is the exchange of water molecules between droplets. Evidence for interdroplet exchange of water has been reported in some microemulsion systems by measurements of time-resolved luminescence quenching.[1,26,48−51] We will evaluate the effect of water exchange as a diffusion coefficient ($D_{exchange}$) using D_{water} and $D_{droplet}$.

Evaluation of the Exchange Rate of Water between Droplets. To estimate $D_{exchange}$, we assume that $D_{exchange}$ is described as the difference between D_{water} and $D_{droplet}$ as

$$D_{exchange} \equiv D_{water} - D_{droplet} \tag{6}$$

Combining the Arrhenius-type thermal activation process and the memory effect described by eq 5, we produce a new equation describing dependence of $D_{droplet}$ on temperature (T) and the water droplet fraction (Φ):

$$D_{droplet} = D_0(1 - 2\Phi) \exp(-E_a/RT) \tag{7}$$

Inserting eq 7 into eq 6, we obtain an equation for $D_{exchange}$. Figure 10 shows $D_{exchange}$ results. Figure 10 indicates that dependence of $D_{exchange}$ on Φ differs from that on temperature. At 295.2 K, which is below T_p, $D_{exchange}$ increases with an increase in Φ. It follows that the frequency of the collisions and the chance of mass exchange between the droplets increase as the number density of the droplets increases. The $D_{exchange}$ value increases for $\Phi < 0.2$ at 317.6 K, which is above T_p, but it remains constant for $\Phi > 0.2$. A reasonable inference is that the rate of the water exchange between droplets is independent of Φ in the region of $0.287 \le \Phi \le 0.605$. This region is above T_p as seen in Figure 1; therefore certain migration paths of the water molecules preexist by formation of aggregation clusters of the droplets and frequent droplet collisions. At the high Φ region, the droplets themselves obstruct diffusion of the droplets. For that reason, eq 7 is true under the condition that $\Phi \ll 1$. Applying eq 7 to the whole volume fraction region up to Φ = 0.605 may overestimate $D_{droplet}$; similarly, use of eq 6 at the higher region of Φ engenders underestimation of $D_{exchange}$. However, Φ dependence of $D_{exchange}$ depends on temperature. This suggests that the obstruction effect at the high Φ region is negligible in this case.

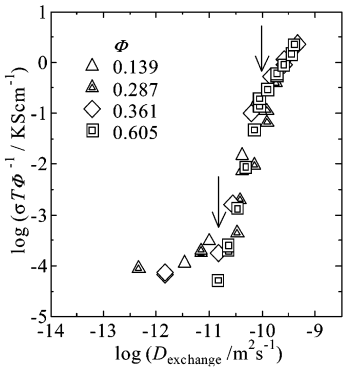

Figure 11. Relation between the scaled conductivity $\sigma T\Phi^{-1}$ and $D_{exchange}$ of water. A scaling relation observed for $\Phi = 0.139$, 0.287, 0.361, and 0.605 is estimated as $\sigma T\Phi^{-1} \sim (D_{exchange})^{\beta}$ [$\beta = 3.2$ for $-10.7 \leq \log(D_{exchange}) \leq -10.0$ and $\beta = 1.3$ for $-10.0 \leq \log(D_{exchange}) \leq -9.3$].

Relation between Electrical Conductivity (σ) and the Diffusion Coefficient for Water Exchange ($D_{exchange}$) in the Entire System. Equation 4, as $\sigma/\Phi = (c/\Phi)(z^2F^2/RT)D$, is useful to discuss the relation between specific electrical conductivity (σ/Φ) and the diffusion coefficient for water exchange between droplets ($D_{exchange}$). In this report, the molar ratio of D_2O and AOT is fixed at $[D_2O]/[AOT] = 40.8$. Therefore the amount of AOT molecules is proportional to the volume fraction of water droplets in the microemulsion (Φ). Thus the relation between σ and D is described as

$$(\sigma/\Phi)T \propto D \tag{8}$$

In this case, D is the diffusion coefficient of the charge carrier. When the exchange of water between the droplets causes the transfer of charge carriers during the fusion and fission processes of the droplets, D in eq 8 could be substituted for $D_{exchange}$. Thereby, deviation of the relation between $(\sigma/\Phi)T$ and $D_{exchange}$ from eq 8 provides detailed information on the transport mechanism of the charge carrier and water exchange between the droplets.

Figure 11 shows $\log(\sigma T\Phi^{-1})$ against $\log(D_{exchange})$ over the whole range of Φ and T. This indicates that all data representing the conduction percolation ($\Phi \geq 0.139$) fall on a single line irrespective of the temperature and the magnitude of the volume fraction in the region where $\log(D_{exchange}) \geq -10.7$; this suggests a distinct scaling relation between σ and $D_{exchange}$. This scaling relation implies that both the conductivity percolation and the exchange of the water between droplets for each Φ are governed by a common mechanism.

Furthermore, Figure 11 shows a change in the slope at $\log(D_{exchange}) \sim -10.0$, suggesting alternation of the conduction mechanism at that point. That scaling relation is thus written as

$$(\sigma/\Phi)T \propto (D_{exchange})^{\beta} \tag{9a}$$

where

$$\beta = 3.2 \qquad \text{for } -10.7 \leq \log(D_{exchange}) \leq -10.0 \tag{9b}$$

and

$$\beta = 1.3 \qquad \text{for } -10.0 \leq \log(D_{exchange}) \leq -9.3 \tag{9c}$$

Deviation of β from unity indicates deviation of the transport process of the charge carrier from a simple diffusion mechanism.

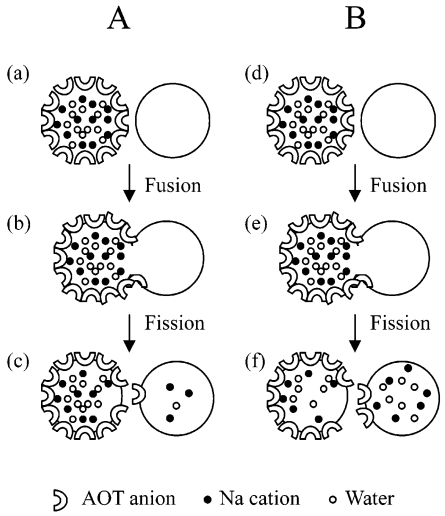

Figure 12. Schematic diagram of the exchange process [fusion (a, d), mass exchange (b, e), and fission (c, f)] between two droplets (large circles). In the left droplet, open (○) and closed circles (●) indicate water molecules and Na cations, respectively; arch-shape figures indicate AOT anions at the droplet surface. For simplicity, the water molecules, Na cations, and AOT anions, which are originally included in the right droplets, are not shown. (A) In the case of a lower frequency and a shorter duration of the exchange process, total numbers of water molecules and the Na cations are fewer, and the Na cations near the surface of droplets are likely to be transferred to another droplet. A small amount of AOT anions at the droplet surface are also transferred. (B) In the case of a higher frequency and a longer duration of the exchange process, the total numbers of water molecules and Na cations are larger and both water and the Na cations can be transferred to another droplet. The AOT anions are also transported.

This is true because β is 1 in the case of the Einstein equation in which the charge conduction and charge carrier motion are related linearly.

The exponent $\beta > 1$ indicates that the exchange of charge carrier between droplets occurs more frequently and effectively than the exchange of water molecules between droplets. Quantitative interpretation of a detailed mechanism of this deviation is difficult. However, one probable qualitative interpretation is made with distribution of the Na cation in a droplet. In a droplet, most Na cations are distributed near the SO_3^- headgroups of the AOT anion.[32,52,53] Therefore, concentration of the Na cations is higher near the droplet surface than in the water droplet interior (Figure 12a,d). For simplicity, Figure 12 does not show the water molecules, Na cations, and AOT anions that are originally included in the right droplets. As depicted in Figure 5, the onset of the increase of D_{AOT} on heating is about 10 K higher than those of D_{water} and σ, indicating that the contribution of AOT anions to σ is negligible far below T_p. In contrast, the contribution of the AOT anion to σ is about 6−21% above T_p. Thus, a small contribution of the AOT anions to σ is expected in the vicinity of T_p.

When fusion of the droplets occurs simultaneously below T_p (Figure 12b), the frequency and duration of collisions are considered to be too small and too short to cause complete exchange of the contents of both droplets. So when fission (Figure 12c) or recovery of the droplets is realized after a mutual collision, small amounts of water molecules, Na cations, and AOT anions traverse from one droplet to the other; however, most water molecules and ions remain in the original droplet. This small number of the ions transferred from one droplet to the other account for the relatively low conductivity (σ) and small diffusion coefficient of water. Moreover, uneven distribution of Na^+ near the droplet surface causes more effective

transfer of Na cations near the surface of one droplet to another than transfer from the droplet interior. The exponent $\beta = 3.2$ in the region $-10.7 \leq \log(D_{\text{exchange}}) \leq -10.0$ implies that Na cation transport efficiency could be higher by about 150 times that of water below the percolation threshold.

On the other hand, in the range $-10.0 \leq \log(D_{\text{exchange}}) \leq -9.3$, which corresponds to the region above T_p, where conduction properties are described as a static percolation, droplet fusion and water exchange between droplets may occur frequently to change droplet contents (Figure 12e). After fission, water molecules and Na cations revert to their original distribution in the droplets (Figure 12f). The numerous transferred Na cations and water molecules account for the high electrical conductivity and the rapid water diffusion, respectively. The less numerous AOT anions also contribute to electrical conductivity. The effect of uneven distribution of Na cation in a droplet almost disappears as a result of very frequent collisions and mass exchange between droplets. Sufficient time exists for water molecules to move between the droplets, yielding a nearly linear relation for conductivity and water exchange as $(\sigma/\Phi)T \propto (D_{\text{exchange}})^{1.3}$. These results suggest that, near T_p and above T_p, electrical conduction and molecular diffusion are both produced by a single event: the exchange of droplet contents.

Conclusions

The scaling relation between $(\sigma/\Phi)T$ and D_{exchange} confirmed that a common mechanism governs conduction percolation and diffusion of water molecules in the AOT-based W/O microemulsion: content exchange between the droplets. Analysis of the scaling relation revealed the detailed mechanism of mass exchange between two droplets, resulting mainly from Na cation distribution inside the droplets. Moreover, we validated the use of PGSE-NMR technique to study the detailed mechanism of conduction properties in W/O microemulsion systems.

Acknowledgment. H.K. thanks Dr. Keonil Lee and Professor Hitoshi Yamamoto for their stimulating discussions of structure and properties of water droplets in a microemulsion system.

References and Notes

(1) Moulik, S. P.; Paul, B. K. *Adv. Colloid Interface Sci.* **1998**, *78*, 99.
(2) Chen, S. H. *Annu. Rev. Phys. Chem.* **1986**, *37*, 351.
(3) Zulauf, M.; Eicke, H.-F. *J. Phys. Chem.* **1979**, *83*, 480.
(4) Day, R. A.; Robinson, B. H.; Clarke, J. H. R.; Doherty, J. V. *J. Chem. Soc., Faraday Trans. 1* **1979**, *75*, 132.
(5) Cabos, C.; Delord, P. *J. Appl. Crystallogr.* **1979**, *12*, 502.
(6) Huang, J. S.; Kim, M. W. *Phys. Rev. Lett.* **1981**, *47*, 1462.
(7) Kotlarchyk, M.; Chen, S. H.; Huang, J. S. *J. Phys. Chem.* **1982**, *86*, 3273.
(8) Assih, T.; Larche, F.; Delord, P. *J. Colloid Interface Sci.* **1982**, *89*, 35.
(9) Kotlarchyk, M.; Chen, S. H.; Huang, J. S.; Kim, M. W. *Phys. Rev. A* **1983**, *28*, 508.
(10) Kotlarchyk, M.; Chen, S. H.; Huang, J. S.; Kim, M. W. *Phys. Rev. A* **1984**, *29*, 2054.
(11) Kotlarchyk, M.; Chen, S. H.; Huang, J. S.; Kim, M. W. *Phys. Rev. Lett.* **1984**, *53*, 941.
(12) Kotlarchyk, M.; Huang, J. S.; Chen, S. H. *J. Phys. Chem.* **1985**, *89*, 4382.
(13) Chen, S. H.; Huang, J. S. *Phys. Rev. Lett.* **1985**, *55*, 1888.
(14) Kotlarchyk, M.; Chen, S. H.; Huang, J. S. *J. Phys. Chem.* **1987**, *91*, 3306.
(15) Bhattacharya, S.; Stokes, J. P.; Kim, M. W.; Huang, J. S. *Phys. Rev. Lett.* **1985**, *55*, 1884.
(16) van Dijk, M. A. *Phys. Rev. Lett.* **1985**, *55*, 1003.
(17) Kim, M. W.; Huang, J. S. *Phys. Rev. A* **1986**, *34*, 719.
(18) Cametti, C.; Condastefano, P.; Tartaglia, P.; Rouch, J.; Chen, S. H. *Phys. Rev. Lett.* **1990**, *64*, 1461.
(19) Chen, S. H.; Rouch, J.; Sciortino, F.; Tartaglia, P. *J. Phys.: Condens. Matter* **1994**, *6*, 10855.
(20) Stauffer, D.; Aharony, A. *Introduction to Percolation Theory*, 2nd ed.; Taylor & Francis: London and Washington, DC, 1992.
(21) Grest, G. S.; Webman, I.; Safran, S. A.; Bug, A. L. R. *Phys. Rev. A* **1986**, *33*, 2842.
(22) Huang, J. H.; Safran, S. A.; Kim, M. W.; Grest, G. S.; Kotlarchyk, M.; Quirke, N. *Phys. Rev. Lett.* **1984**, *53*, 593.
(23) Hilfiker, R.; Eicke, H.-F.; Geiger, S.; Furler, G. *J. Colloid Interface Sci.* **1985**, *105*, 378.
(24) Peyrelasse, J.; Moha-Quchane, M.; Boned, C. *Phys. Rev. A* **1988**, *38*, 904.
(25) Maitra, A.; Mathew, C.; Varshney, M. *J. Phys. Chem.* **1990**, *94*, 529.
(26) Jada, A.; Lang, J.; Zana, R. *J. Phys. Chem.* **1989**, *93*, 10.
(27) Jada, A.; Lang, J.; Zana, R. *J. Phys. Chem.* **1990**, *94*, 381.
(28) Dutkiewicz, E.; Robinson, B. H. *J. Electroanal. Chem.* **1988**, *251*, 11.
(29) Mukhopadhyay, L.; Bhattacharya, P. K.; Moulik, S. P. *Colloids Surf.* **1990**, *50*, 295.
(30) Feldman, Y.; Kozlovich, N.; Nir, I.; Garti, N.; Archipov, V.; Idiyatullin, Z.; Zuev, Y.; Fedotov, V. *J. Phys. Chem.* **1996**, *100*, 3745.
(31) Eicke, H.-F.; Christen, H. *J. Colloid Interface Sci.* **1974**, *48*, 281.
(32) Wong, M.; Thomas, J. K.; Nowak, T. *J. Am. Chem. Soc.* **1977**, *99*, 4730.
(33) Fedotov, V. D.; Zuev, Y. F.; Archipov, V. P.; Idiyatullin, Z. S. *Appl. Magn. Reson.* **1996**, *11*, 7.
(34) Stejskal, E. O.; Tanner, J. E. *J. Chem. Phys.* **1965**, *42*, 288.
(35) Hait, S. K.; Moulik, S. P.; Palepu, R. *Langmuir* **2002**, *18*, 2471.
(36) Stauffer, D. *Phys. Rep.* **1979**, *54*, 1.
(37) Sheu, E. Y.; Chen, S. H.; Huang, J. S.; Sung, J. C. *Phys. Rev. A* **1989**, *39*, 5867.
(38) Huang, J. S.; Sung, J.; Wu, X.-L. *J. Colloid Interface Sci.* **1989**, *132*, 34.
(39) Huang, J. S.; Kotlarchyk, M. *Phys. Rev. Lett.* **1986**, *57*, 2587.
(40) Mills, R. *J. Phys. Chem.* **1973**, *77*, 687.
(41) Kataoka, H. Doctoral Thesis, Osaka University, Osaka, Japan, 1997.
(42) Eicke, H.-F.; Hilfiker, R.; Holz, M. *Helv. Chim. Acta* **1984**, *97*, 361.
(43) Geiger, S.; Eicke, H.-F. *J. Colloid Interface Sci.* **1986**, *110*, 181.
(44) Ackerson, B. J. A.; Fleishiman, L. *J. Chem. Phys.* **1982**, *76*, 2675.
(45) Hanna, S.; Hess, W.; Klein, R. *Physica A* **1982**, *111*, 181.
(46) Lekkerkerker, H. N. W.; Dhont, J. K. G. *J. Chem. Phys.* **1984**, *80*, 5790.
(47) Berg, R. F.; Moldover, R.; Huang, J. S. *J. Chem. Phys.* **1987**, *87*, 3687.
(48) Fletcher, P. D. I.; Howe, A. M.; Robinson, B. H. *J. Chem. Soc., Faraday Trans. 1* **1987**, *83*, 985.
(49) Jada, A.; Lang, J.; Zana, R.; Makhloufi, R.; Hirsh, E.; Candau, S. *J. Phys. Chem.* **1990**, *94*, 387.
(50) Almgren, M.; Jóhannsson, R. *J. Phys. Chem.* **1992**, *96*, 9512.
(51) Mays, H.; Ilgenfritz, G. *J. Chem. Soc., Faraday Trans.* **1996**, *92*, 3145.
(52) Tomić, M.; Kallay, N. *J. Phys. Chem.* **1992**, *96*, 3874.
(53) Kozlovich, N.; Puzenko, A.; Alexandrov, Y.; Feldman, Y. *Colloids Surf. A: Physicochem. Eng. Aspects* **1998**, *140*, 299.